

10

Supplementary Information

Experimental and simulated SAED patterns of $\text{Li}_7\text{La}_3\text{Zr}_2\text{O}_{12}$ in [001] viewing direction are shown in Fig. SX1. There are almost no differences in the diffracted intensities for the SAED patterns.

The differences in the “*a*” parameter between cubic and tetragonal $\text{Li}_7\text{La}_3\text{Zr}_2\text{O}_{12}$ amount to only 1.5% which is the accuracy limit of the SAED measurements. Thus, the distinction between two modifications is impossible only from one SAED image.

15

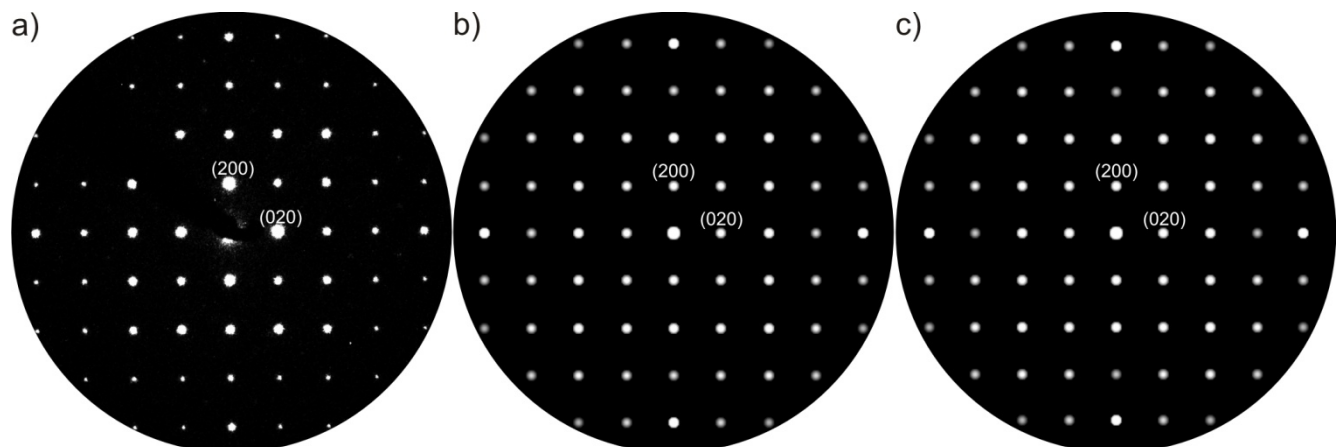


Fig. SX1 (a) Experimental SAED pattern of cubic $\text{Li}_7\text{La}_3\text{Zr}_2\text{O}_{12}$ and simulated SAED patterns of (b) cubic $\text{Li}_x\text{La}_3\text{Zr}_2\text{O}_{12}$ and (c) tetragonal $\text{Li}_7\text{La}_3\text{Zr}_2\text{O}_{12}$ along [001] viewing direction.

20

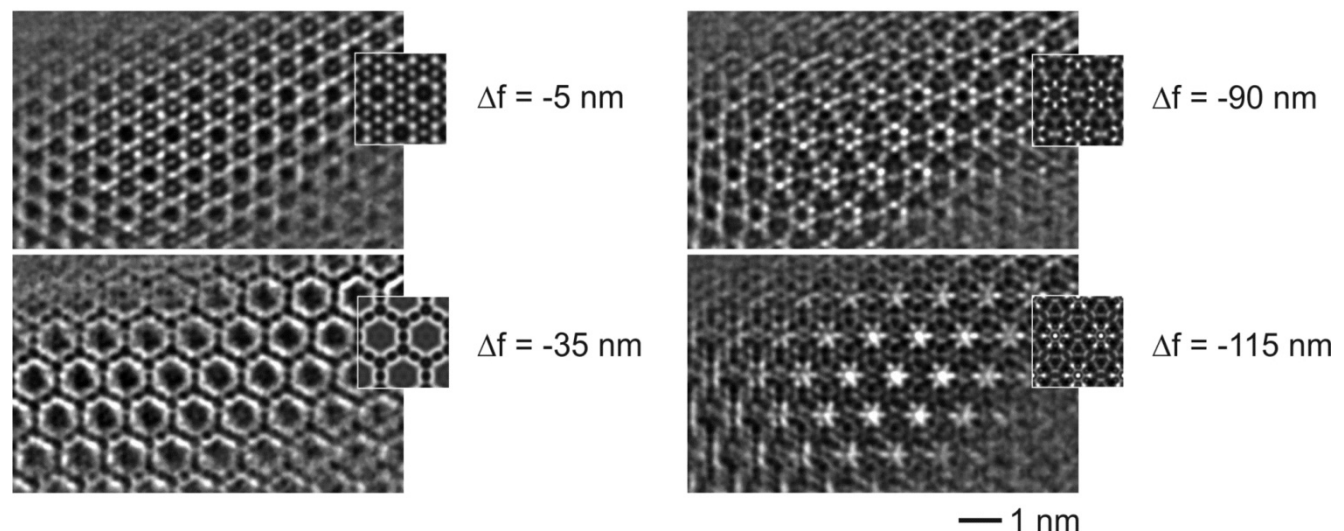


Fig. SX2 Complete focal series for $\text{Li}_7\text{La}_3\text{Zr}_2\text{O}_{12}$ with inserted simulated micrographs (zone axis [111], $t = 6.7 \text{ nm}$). Focus values specified in the figure.

25

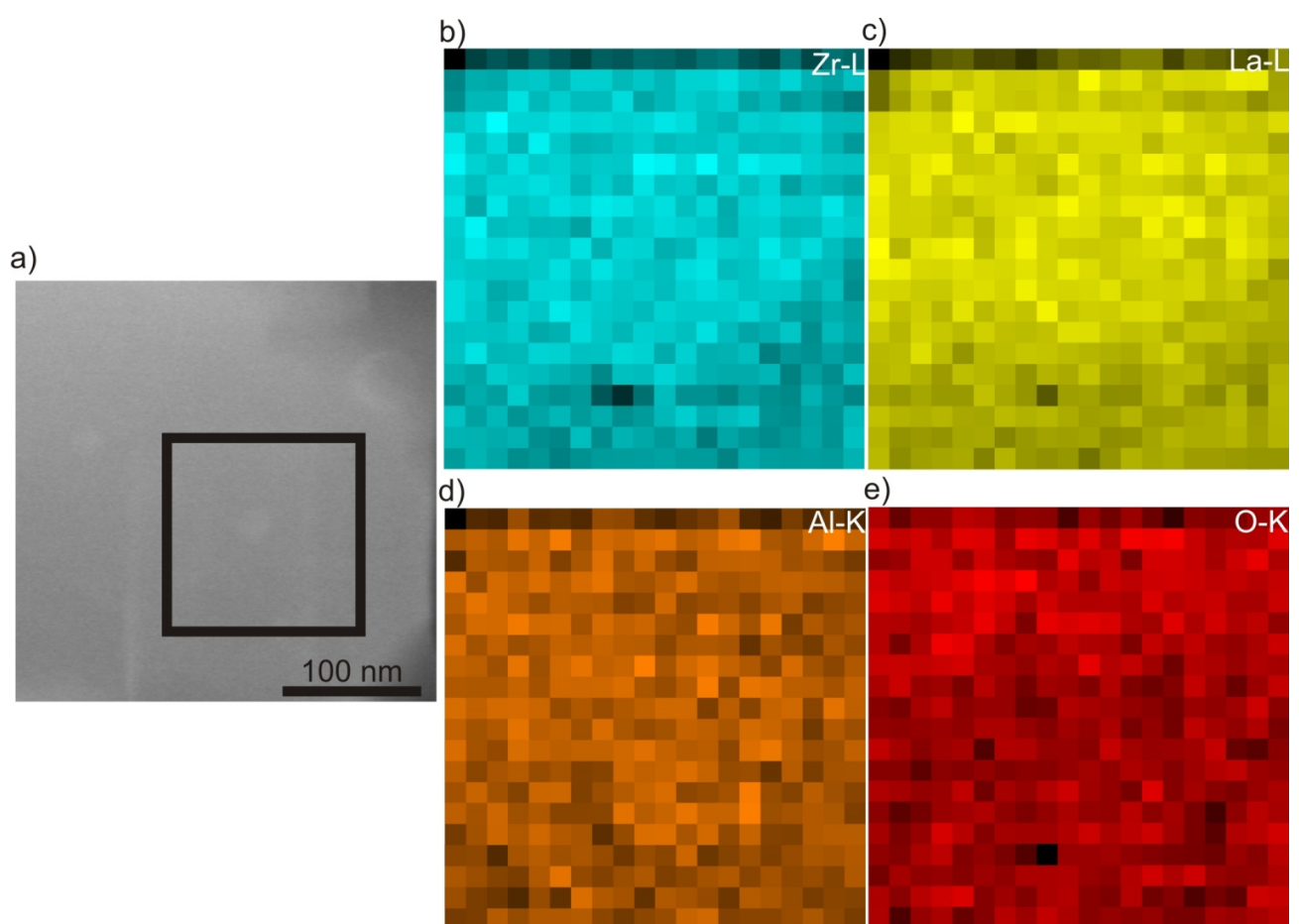


Fig. SX3 (a) STEM-HAADF image and (b)-(e) STEM EDX elemental maps of LLZO sample containing 0.9 wt.% of Al.